Journal of Molecular Structure 1228 (2021) 129701

Contents lists available at ScienceDirect

Journal of Molecular Structure

journal homepage: www.elsevier.com/locate/molstr

Colorimetric sensing and anion recognition by *Kalanchoe* flower-like ligand and its transition metal complexes with polarized N-H interaction motifs

A. Kosiha[a,*], M. Devendiran[b], K. Krishna Kumar[b], R.A. Kalaivani[a]

[a] *Department of Chemistry, School of Basic Science, Vels Institute of Science, Technology & Advanced Studies (VISTAS)(Deemed to be University), Chennai 600 117, India*

[b] *Central Instrumentation Laboratory, Vels Institute of Science, Technology & Advanced Studies (VISTAS)(Deemed to be University), Chennai 600 117, India*

ARTICLE INFO

Article history:
Received 4 May 2020
Revised 12 November 2020
Accepted 30 November 2020
Available online 3 December 2020

Keywords:
Anion sensing
DFT
Fluoride ion
kalanchoe flower-like ligand
N-H interaction motifs

ABSTRACT

Herein we report the selective sensing of fluoride ion with *kalanchoe flower*-like **ligand, L** (2–chloro–3–((3–dimethylamino)propylamino)naphthalene–1,4–dione) and it's metal (**K1-Cu(II), K2-Co(II), K3-Zn(II)**) complexes. The morphology and anion sensing properties of the L and K1-K3 compounds were investigated with microscopic and spectroscopic techniques. ^{1}H NMR titration was carried out to understand the fluoride ion interaction with the N-H interacting site of the ligand and its metal complexes. Furthermore, quantum chemical calculations were conducted to rationalize the interaction between chemosensors and anions.

1. Introduction

Quinone derivatives signify a large group of substances present in several families of plants and microorganisms. They enact key roles in vital processes such as cellular respiration and photosynthesis due to its facile electron transfer property. Quinones are classified as benzoquinones, naphthoquinones, and anthraquinones based on aromatic systems [1,2]. Though quinones imprinted their promising anticancer activities, tailoring with naphthaquinone derivatives exhibit diverse pharmacological properties and potential anticancer activities [3]. In particular 1,4-naphthoquinone demonstrates important anticancer activity in several drugs, such as streptonigrin, mitomycin, and actinomycin, [4]. It is worth to note that 2,3-dichloronaphthoquinone is key synthetic intermediate in organic, medicinal, and industrial chemistry. In this study, the synthesized ligand was used to make CT (charge transfer) complexes by external electron donors. In this phenomenon, the amine group is formed between a weak nucleophile, the ligand precursor 2,3-dichloronaphthoquinone, and dimethyl propylene diamine [5–7]. The biological activity of quinone enhances when it is coordinated to transition metal ions [8]. The design and development of anion recognizing motifs gain much attention in the research areas of supramolecular chemistry, environmental ecosystem, and diagnostic tool in medicinal fields due to its selectivity and sensitivity [9]. Some of the anions like phosphate, fluoride, cyanide, and nitrate are convicted as pollutants due to their harmful roles. Among these, a great deal of attention is devoted to the development of chemosensors for the basic anion of fluoride recognition and real-time monitoring because of its clinical treatments for osteoporosis, orthodontics. The excess of fluoride entry into the body leads to adverse effects like fluorosis and urolithiasis [10–12]. Fluoride ion sensing motifs occur in hydrogen bonding units such as triarylboranes, desilylation, pyrroles, amides, ureas, thioureas or sulphonamides [9] and are available in the literature. Sensing motifs are developed based on NH deprotonation or hydrogen bond formation with F^- ion which has been reported for the selectivity of F^- ions over the other competitive anions [12,13]. Synthesis, spectral characterization, and their biological activity of **L** and **K1-K3** compounds were reported earlier [14]. In the present study, the selective colorimetric sensing of fluoride anion with the naphthoquinone **L** and **K1-K3** compounds was reported.

2. Experimental methods

2.1. Chemicals

All the anions as their tetrabutylammonium salts, solvents, and other chemicals were purchased from Sigma-Aldrich and

* Corresponding author.
E-mail address: kosiha@gmail.com (A. Kosiha).

https://doi.org/10.1016/j.molstruc.2020.129701
0022-2860/

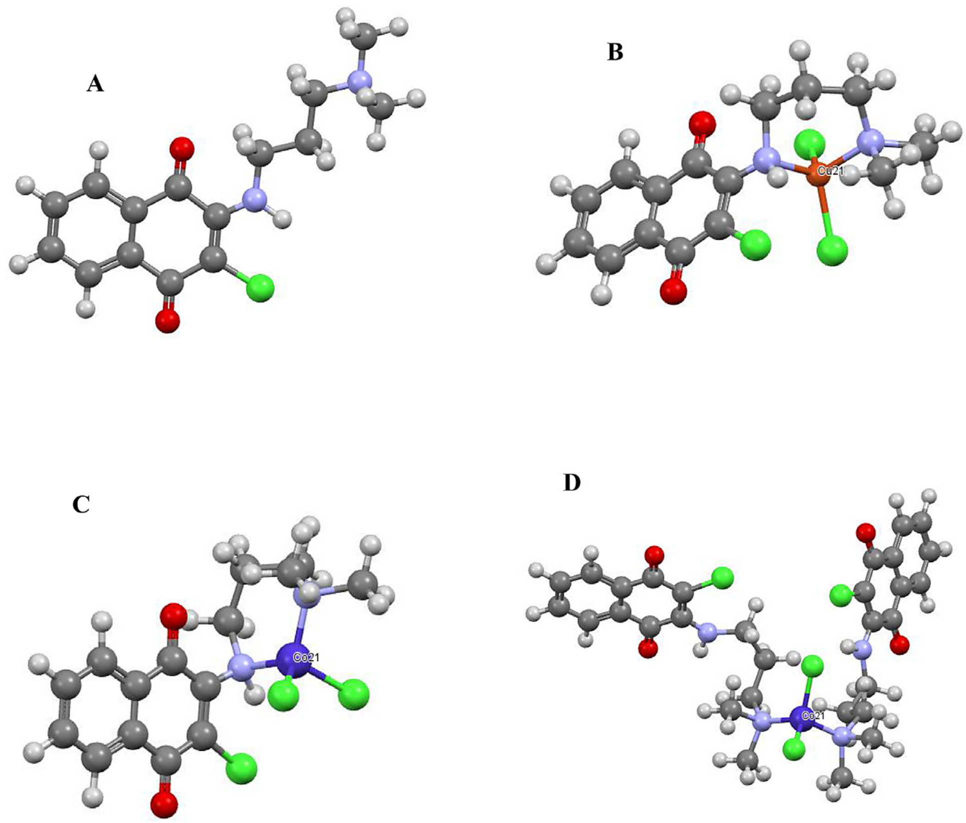

Fig. 1. Optimized Structures of **L** (**A**), **K1** (**B**), **K2** (**C**) and **K3** (**D**).

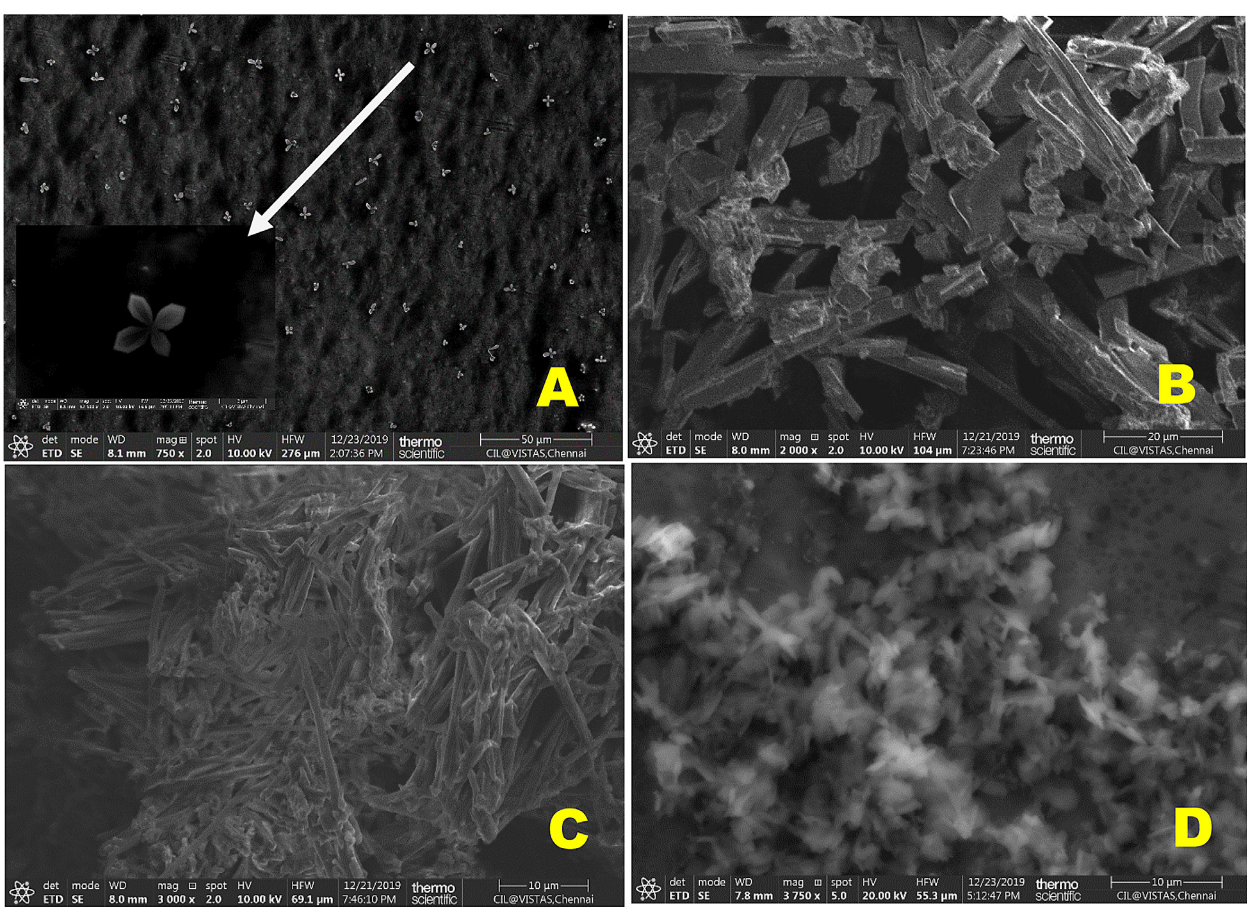

Fig. 2. FESEM images for **L** (**A**) (Inset: Magnified image), **K1** (**B**), **K2** (**C**) and **K3** (**D**).

Merck (India). The precursor, chemosensor ligand **(L)** (2–chloro–3–((3–dimethylamino)propylamino)naphthalene–1,4–dione) and **K1-K3** complexes, were prepared as reported in our previous paper [14].

2.2. Instrumentation

The absorption spectra were carried out on JASCO (V630, Japan) double beam spectrophotometer, while fluorescence spectra were on the Caryeclipse fluorescence spectrophotometer (Agilent technologies). Nuclear magnetic resonance spectra were recorded on Bruker, 300 MHz spectrometer in presence of DMSO-d_6 solvent using tetramethylsilane (TMS) as internal reference. The chemical shift were expressed in units of ppm (normalized integration, multiplicity, and the value of J in Hz) with respect to the DMSO-d_6. ^{1}H NMR titration studies were carried out with incremental addition of (0.5 and 1eq.) F^- to the DMSO-d_6 solution of **L** and **K3.** Surface morphology investigation was done using the Thermo Scientific QuattroS field emission scanning electron microscope (FESEM). The geometrical optimization of the complexes was performed using Density Functional Theory with the B3LYP hybrid functional, by using a basis set of 6-31G. Computations have been performed using the Gaussian 03 Revision D.01 program package.

2.3. Synthesis of the L and K1-K3

The **L** and **K1-K3** were synthesized and characterized by using various analytical methods as mentioned in our previous work [14]. In brief, an ethanolic solution of 2,3-dichloro-1,4-naphthoquinone (DCNQ) (5g, 0.0220 mol) and N,N'-dimethylpropylenediamine (6.15g, 0.0220 mol) was stirred at RT for 4 h, resulting in the precipitation of solid product. It was washed with 50% ethyl acetate and pet ether. Then it was dissolved in water, neutralized with potassium carbonate and obtained as pure product after dried.

Ligand (1.7 mmol) was dissolved in 10 mL of dichloromethane (DCM) and then metal chloride salts (1.7 mmol) dissolved in 10 mL of ethanol was added drop-wise, stirred and heated at 50°C for 5 h [14]. After the evaporation of all the solvents, the solid product collected was washed with DCM and ethyl acetate. The optimized structures of **L, K1, K2,** and **K3** have been depicted in Fig. 1.

3. Results and Discussion

3.1. Structure Characterization

The chemical structure of **L** was confirmed by elemental and spectral analyses. The IR spectrum of **L** exhibits the characteristic peaks at 3433 υ(NH), 1595 and 1679cm^{-1} pro to υ(C=O) which confirms the structure of the ligand. The molecular structure of **L** was also determined by X-ray crystallography. The compounds **K1-K3** were prepared in high yields in single step reaction. The structural identities of **K1-K3** were also characterized by FT-IR, UV–vis, ESR spectroscopy, HR-MS technique, thermal analysis (TGA), and magnetic moment measurements(Figure S1-S8 and Table S1,S2) [14].

3.2. Morphological study

The surface morphology of the **L** and **K1-K3** compounds was studied by using a Field emission scanning electron microscope (FESEM) under Environmental Scanning Electron Microscopy (ESEM) mode. Fig. 2 shows the FESEM surface morphology of all the compounds. The **L** was distributed uniformly as shown in Fig. 2A and resembles a *kalanchoe flower* (four-leaf flower) like structure. The micrograph of **K1** shows the formation of loosely aggregated rods (Fig. 2B). FESEM image of **K2** has looping stick with fine-sized particles (Fig. 2C) like morphology. Finally, **K3** exhibits a large quantity of flower-shaped nanoflakes aggregation(Fig. 2D). Hence, FESEM micrographs indicated the **L** and **K1-K3** compounds were microns in size [15].

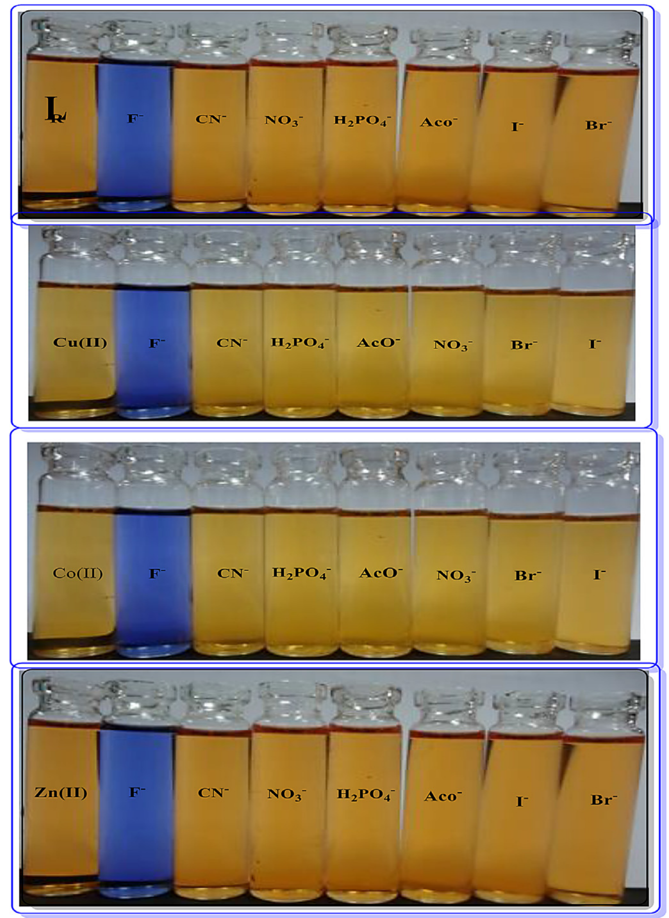

Fig. 3. Color changes of **L, K1, K2 and K3** with anions.

3.3. Anion Sensing

The anion sensing properties of compounds **(L, K1-K3)** were investigated using various techniques such as UV-vis, fluorescence, ^{1}H NMR, and DFT computations to substantiate the spectral conclusions.

3.3.1. Naked-eye detection

The colorimetric sensitivity of **L** and **K1-K3** compounds towards various anions such as F^-, Br^-, I^-, AcO^-, $H_2PO_4^-$, CN^- and NO_3^- in their tetra butyl ammonium form, was monitored visually concomitantly. As shown in the figure (Fig. 3), a color change from yellow to blue was observed upon the addition of fluoride ion to the solution of **L and K1** (in 20% aq. DMF), **K2** and **K3** compounds. At the same time, their color remains unchanged after the addition of Br^-, I^-, AcO^-, $H_2PO_4^-$, CN^- and NO_3^- this is probably due to high negative charge density on F^- which brings out the strong hydrogen bonding with NH in **L** and **K1-K3** compounds [16,17].

3.3.2. UV-vis spectroscopic studies

The interaction of the **L** and **K1-K3** compounds with F^- was investigated in detail through UV-vis spectroscopy in DMF solutions containing 2.5 × 10^{-4}M of the test compounds. The titration was

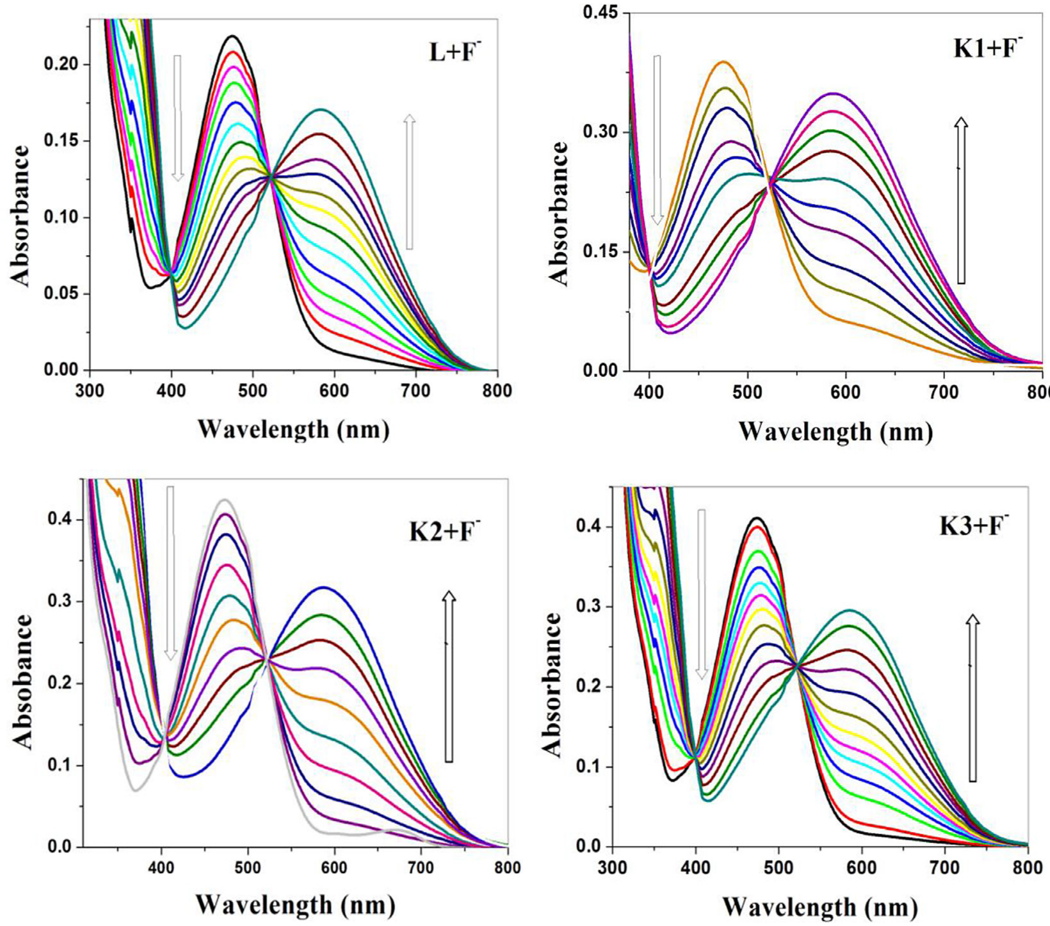

Fig. 4. UV-vis absorbance changes of **L, K1, K2, and K3** upon addition of fluoride ions in DMF.

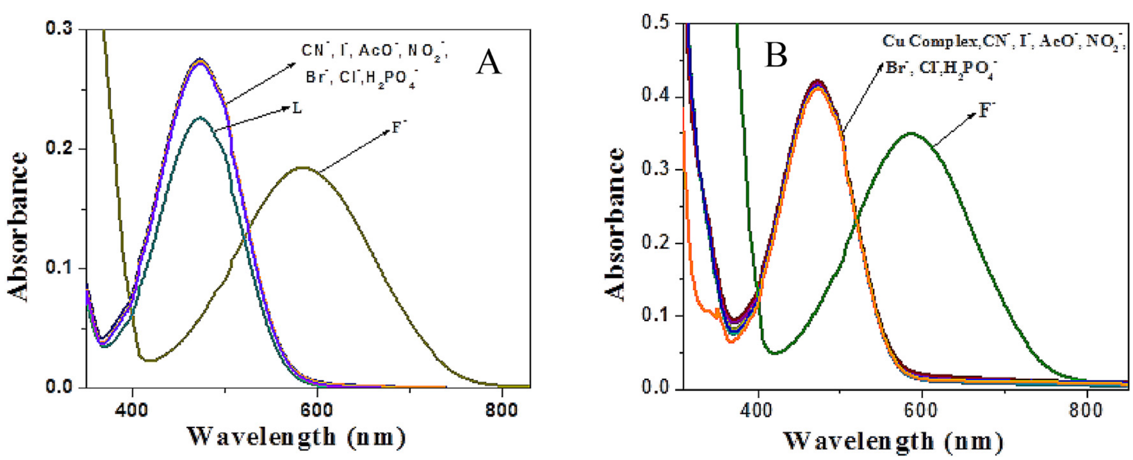

Fig. 5. Other anions with **L** (A) and **K3** (B).

carried out with **L, K1-K3** and their corresponding UV-vis spectral changes are depicted in Fig. 4. With the addition of incremental amounts of fluoride ion to the solution of **L** and **K1-K3,** the absorption spectral peak at λ_{max}474 nm (log ε=2.95), which corresponds to the intramolecular charge transfer (ICT) transition (n-π^*) from N-atoms to the quinone moiety [18] disappears gradually and accompanying the formation of the new band centered at 585 nm (bathochromic shift). The **K1** also exhibited similar spectral behavior on adding fluoride ions (Fig. 5) to the solution of DMF: H_2O (80:20%). This is accompanied by the instantaneous formation of blue color (Δ λ_{ICT}=111nm) with a occurrence of new band due to the ICT transition between the receptor (amine N-H—F^-) and quinone signaling units. Thus, the metal complex is passably a better electron donor than free ligand. The UV-vis spectra of **L** and **K1** compounds were showed no perceptible color change during the addition of other anions except F^- (Fig. 5) and confirmed that the compounds were highly selective towards fluoride ion [19,20]. The stoichiometry of **L** and metal complexes **(K1- K3)** with anions, were studied by continuous variation method (jobs pot) [19]. The proposed complex of compounds with anion stoichiometries is shown in Fig. 6. The **L, K1,** and **K2** with F^- ion seemed to have the binding mole fraction of compounds of 0.5, which means **L** and

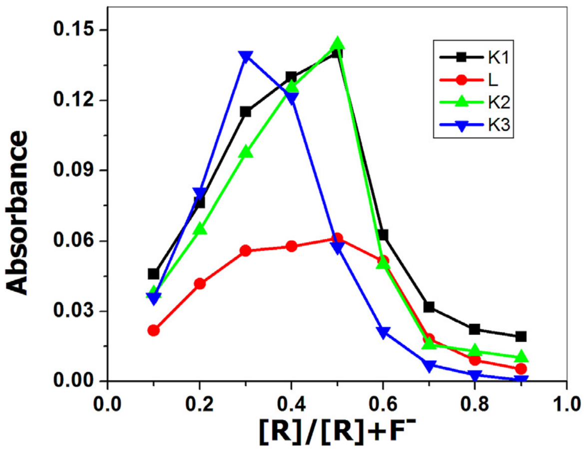

Fig. 6. Job's plot for **L, K1, K2, and K3**.

K1-K3 compounds form a complex with anions at a stoichiometry of 1:1 ratio. The mole fraction of **K3** is 0.3, which means the stoichiometry of **K3** and anion complex is 1:2 ratio [21].

3.3.3. Emission spectral studies

The fluorescence spectroscopy measurements that respond to the ability of **L** and **K1-K3** with fluoride ions were recorded with excitation at 475,472, 472, and 473nm, respectively. As shown in Fig. 7 it is evident that the addition of an incremental amount of F^- to the **L** and **K1-K3** in all cases, the emission intensities of these compounds at 587, 620, 620, and 403 nm respectively were gradually increased. These results indicate that the fluoride ions interact with the **L** and **K1-K3** compounds through H-bonding [22,23].

From the fluorescence enhancement data the binding constant of the **Ligand**-F^- complex can be determined using the Bensi-Hildebrand equation [24].

$$(F_\alpha - F_0)/(F_x - F_0) = 1/k[F^-]$$

Where F_0, F_α, and F_x are the fluorescence response observed in the absence, presence of F^- ion, and at a specific concentration of F^- to complete the interaction, respectively. Fig. 8 shows linear plots of $(F_\alpha$-$F_0)/(F_x$-$F_0)$ versus $1/[F^-]$ for the **L** and **K1-K3**. From the observed enhancement of emission intensity, the binding constant of the compounds -F^- was calculated using the following equation [23]

$$\log (F_o - F)/F = \log K_a + n \log [Q]$$

Where F_0, F fluorescence responses observed in the absence and presence of fluoride ion, at the quencher concentration [Q] and K_a is the binding constant and n is the stoichiometry ratio between the F^- and **L, K1-K3**. The plot of log (F_0 – F) versus log [Q] is linear for F^- with **L, K1, K2,** and **K3** as shown in Fig. 9. The binding constants were calculated to be 4.67×10^4, 2.81×10^5, 1.41×10^5, and 4.81×10^4 for the **L, K1-K3**, respectively. The result of emission study was manifested that the alliance of the **L** and **K1-K3** with fluoride ions are in the sequence of **K1 >K2 >K3> L.** These results anticipated that the complexation process would make the amine hydrogen atom more acidic and inevitably a better H-bond donor towards fluoride ions [25]. The detection limit of **L, K1-K3** for F^- was calculated and showed in Table 1. From that, the lowest detection limit of F^- with **K1** is 2.04 μM.

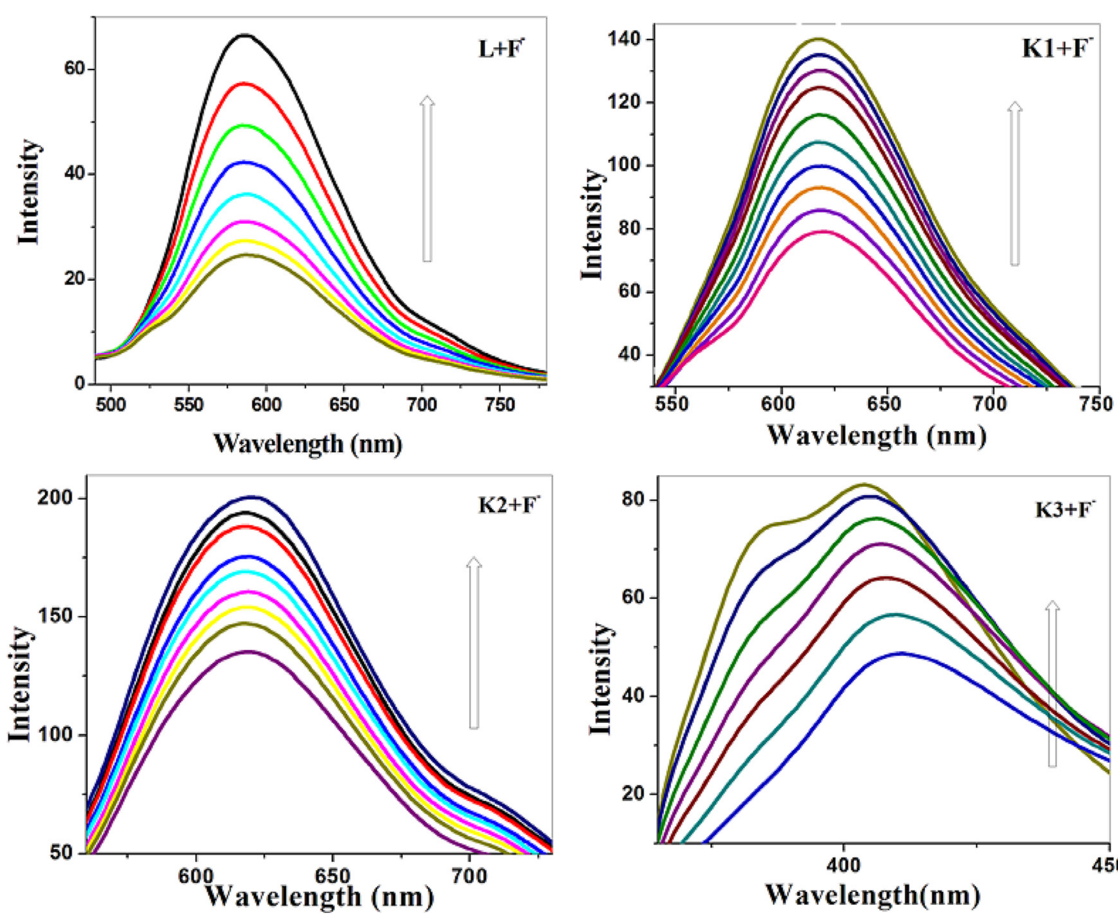

Fig. 7. Fluorescence titration curves of **L, K1, K2, and K3** upon addition of fluoride ion in DMF.

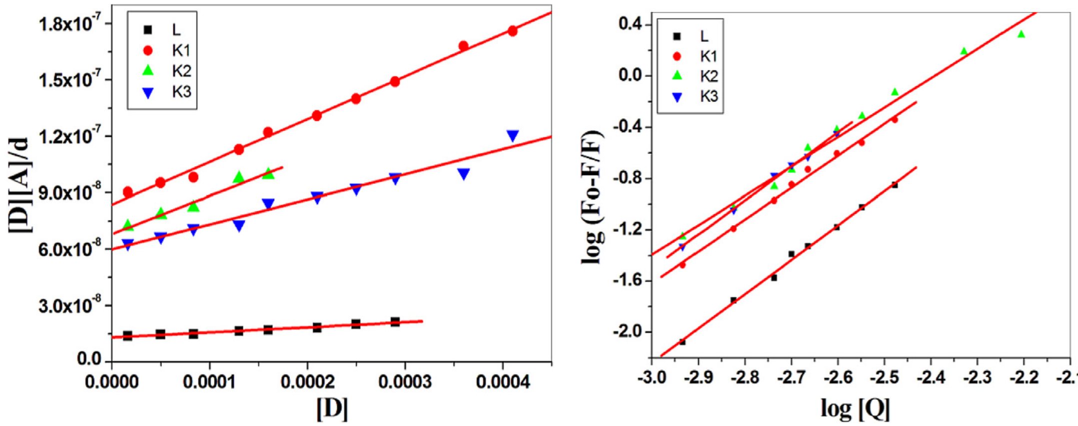

Fig. 8. Benesi-Hildebrand plot used to determine the association constant of the ICT complex formed by and F^- at different fluoride concentrations.

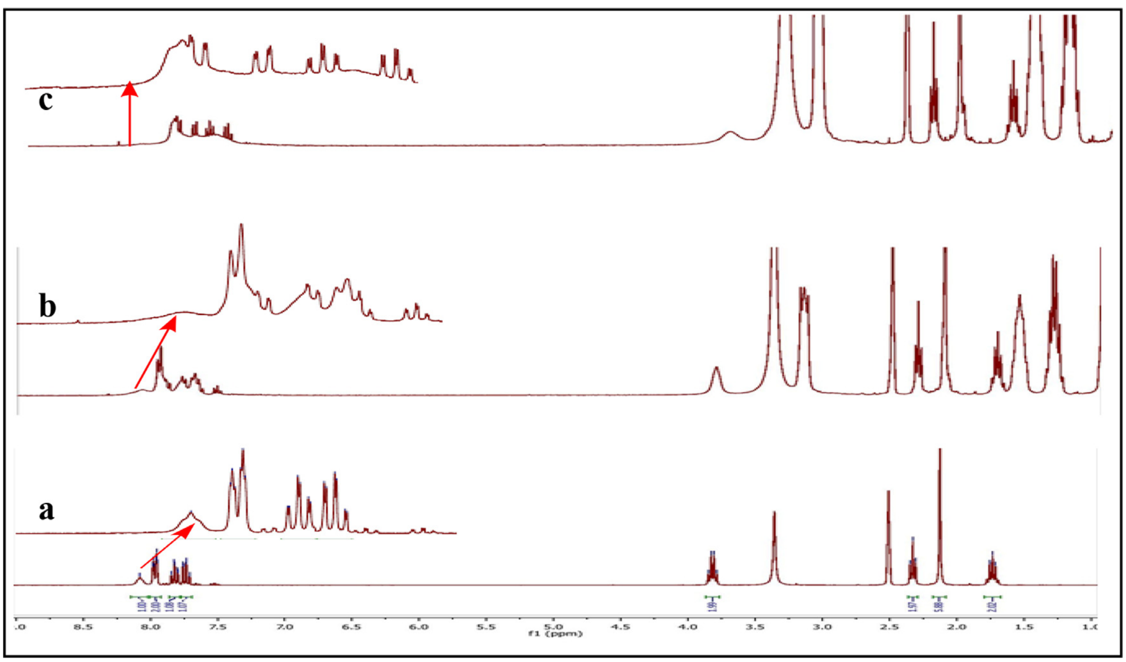

Fig. 9. ^1H NMR spectra of (a)**L** with (b) 0.5, (c) 1 eqv. of F^- ion in DMSO-d_6.

Table 1
Detection Limit, Association and Binding constants (K_A) of ligand and its complex with F^- ions.

Receptor	λ_{ICT} (nm) Without F^-	With F^-	$\Delta\lambda_{ICT}$ (nm)	Association Constant (K_A)/ M^{-1}	λ_{ex} (nm)	λ_{em} (nm)	Binding Constant (K)/mol^{-1}L	Detection Limit (μM)
L	475	585	110	2.43×10^3	475	416	4.67×10^4	68
Cu(II)	472	590	118	5.30×10^3	472	620	2.81×10^5	2.04
Co(II)	472	591	119	3.45×10^3	472	620	1.41×10^5	3.81
Zn(II)	473	587	114	3.22×10^3	473	411	4.81×10^4	27

3.3.4. ^1H NMR titration

The interaction of **L** and **K3** with F^- ion was deliberated with ^1H NMR titration in DMSO-d_6 solvent, which results a significant chemical shift changes on the N-H proton with the addition of F^-ion [26,27]. This was emblematic of strong hydrogen bonding interaction between the N-H group and the anion. Before the addition of F^-, NMR chemical shift, for NH proton was observed at δ 8.08 ppm (in case of L) and δ 8.07 ppm (in case of **K3**). Upon the addition of 0.5 and 1equiv. of F^- to the **L** and **K3**, the characteristic sharp NH peak of sensing motifs were moved to broadening and disappeared finally without disturbing other organic protons as illustrated in Figs. 9 and 10. Surprisingly, we observed broadening of NH in both the **L** and **K1-K3** compounds with F^- was downfield broadening, because F^- causes deshielding of NH proton due to H-bonding that resulted into downfield shifting [23].

3.3.5. Theoretical studies

DFT study calculations were used to monitor and support the photophysical changes of F^- with **L** and **K1-K3** and the energies were compared with experimental observation. The geometries were optimized at DFT based B3LYP/6-31G level of theory [28]. The interaction of F^- with **L** and **K1-K3** was analyzed computationally by predicting frontier molecular orbitals (HOMO and LUMO) along with the difference in energy between them and is

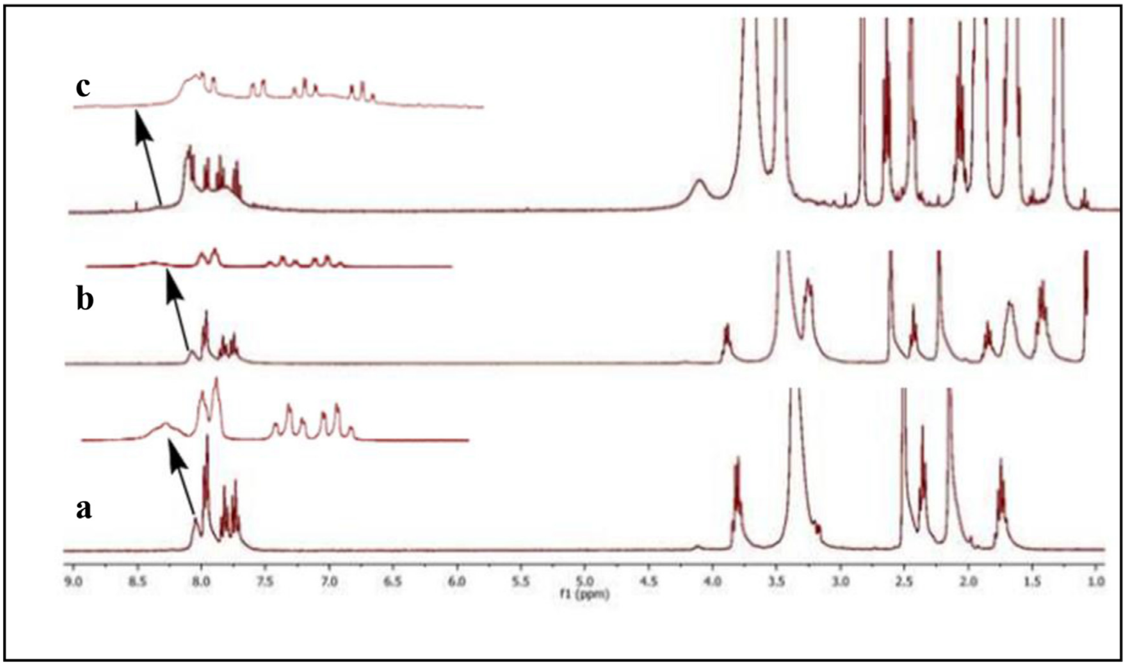

Fig. 10. [1]H NMR spectra of (a) **K3** with (b) 0.5, (c) 1 eqv. of F^- ion in DMSO-d_6.

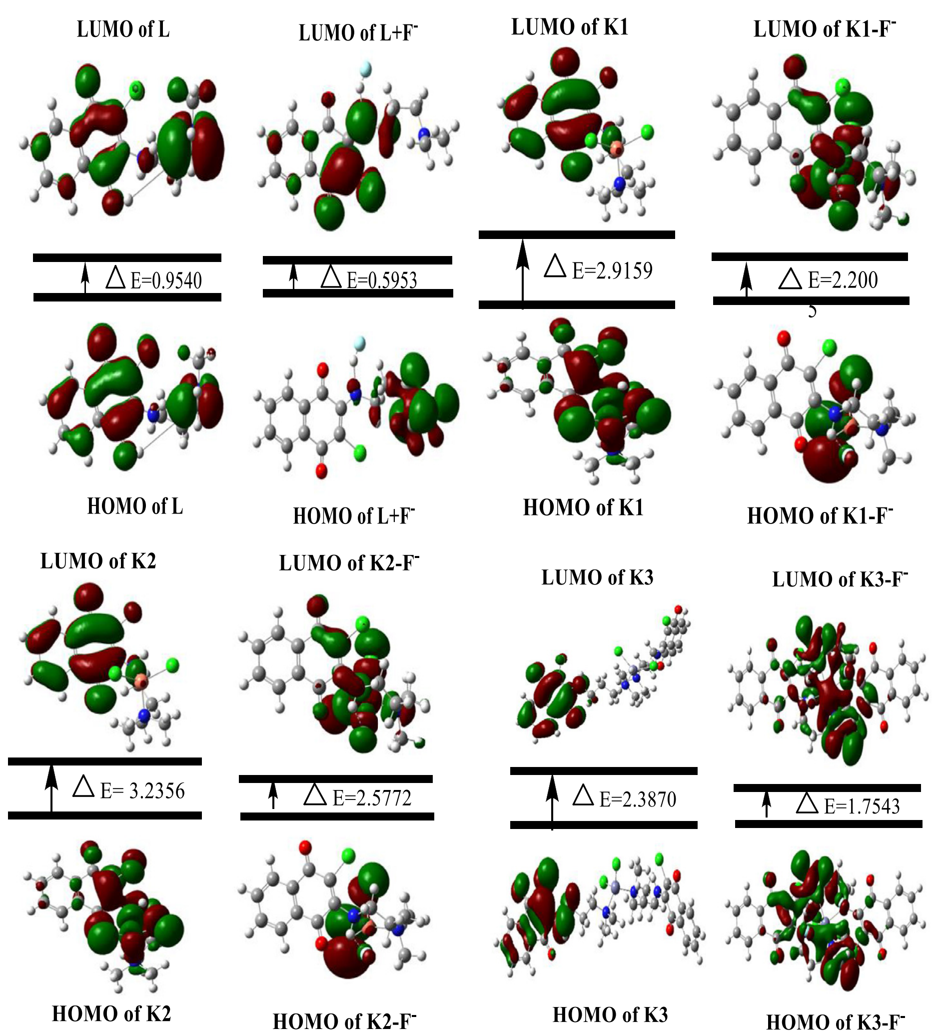

Fig. 11. Frontier MO's of **L, K1, K2, and K3**.

Table 2
Theoretical data of the **L, K1, K2, and K3**.

Compound/Complex	HOMO (eV)	LUMO (eV)	ΔE (eV)
L	5.4564	4.5024	0.9540
L + F^-	3.6937	3.0983	0.5953
Cu(II)	6.6268	3.7108	2.9159
Cu(II)+ F^-	6.3769	4.1764	2.2005
Co(II)	6.0715	3.4943	3.2356
Co(II) + F^-	6.4918	3.9146	2.5772
Zn(II)	5.8292	3.4422	2.3870
Zn(II) + F^-	5.6899	3.9356	1.7543

depicted in Fig. 11. The difference in energy between the HOMO to LUMO ($\Delta E = E_{HOMO} - E_{LUMO}$) of the L was found to be 0.9540eV; these changes are due to intramolecular charge transfer (ICT) observed at 479 nm in the electronic spectrum. The HOMO-LUMO energy gap decreased upon interaction of F^- ion with L and was found to be 0.5953eV (Table 2). This reduction is due to the formation of F^--hydrogen bond. Hence, the inter electron charge transfer transition occurs at a relatively higher wavelength, exhibiting visible color change with the addition of F^- ions. The observed changes may be due to the facile electron donation of N-H—F- site when compared to free N-H site [29,30]. The energy values of both HOMO and LUMO were affected by F^- ion binding with **L** and **K1-K3**. From the results it was found that ΔE for the **K1-K3+F⁻** ion complex is relatively lower than that for the corresponding **L+F⁻** [22]. Moreover, the experimental observations well corroborate with theoretical findings.

4. Conclusion

In summary, the **L, K1-K3** compounds of amine N-H interacting sites encompassing to chromophoric extend quinone moieties, have been investigated towards the anion sensing. The detailed examination based on UV-visible, fluorescence, and ^{1}H NMR spectroscopic determination suggest the interaction of amine N-H site of **L, K1, K2,** and **K3** with anions. Among various anions, the interaction of fluoride ion with **L, K1, K2,** and **K3** compounds can be detected with the naked-eye through color change. UV-vis spectroscopic investigation also unveils the selectivity of the **L, K1, K2,** and **K3** towards F^- ion. Additionally, results of ^{1}H NMR titration have shown hydrogen bonding interactions between -NH groups of the sensing motifs with fluoride anion leads to deprotonation. These studies showed that the ligand and its metal complexes towards the selective determination of F^- and among those, **K1** shows a lower detection limit compared to the **L, K2** and **K3**. Furthermore, DFT calculations also strengthened the experimental data and the proposed sensing mechanisms.

Declaration of Competing Interest

The authors declare that they have no known competing financial interests or personal relationships that could have appeared to influence the work reported in this paper.

CRediT authorship contribution statement

A. Kosiha: Conceptualization, Methodology, Investigation, Writing - original draft. **M. Devendiran:** Formal analysis, Writing - review & editing. **K. Krishna Kumar:** Resources. **R.A. Kalaivani:** Project administration.

Acknowledgement

The authors are thankful to Dr. T. Sathiya Kamatchi, Dr. D S Kothari Post Doctoral Fellow for her timely help to improve the quality of the manuscript.

Supplementary materials

Supplementary material associated with this article can be found, in the online version, at doi:10.1016/j.molstruc.2020.129701.

References

[1] P.R. Kavitha Rani, A. Fernandez, A. George, V.K. Remadevi, M.R. Sudarsanakumar, S.P. Laila, et al., Synthesis, spectral characterization, molecular structure and pharmacological studies of N'-(1, 4-naphtho-quinone-2yl) isonicotinohydrazide, Spectrochim. Acta. A Mol. Biomol. Spectrosc. 135 (2015) 1156–1161, doi:10.1016/j.saa.2014.07.092.

[2] M.J.A. Martinez, P. Bermejo Benito, Biological activity of quinones, Stud. Nat. Prod. Chem. 30 (2005) 303–366, doi:10.1016/S1572-5995(05)80036-5.

[3] V.C. Niculescu, N. Muresan, A. Salageanu, C. Tucureanu, G. Marinescu, L. Chirigiu, et al., Novel 2,3-disubstituted 1,4-naphthoquinone derivatives and their metal complexes - Synthesis and in vitro cytotoxic effect against mouse fibrosarcoma L929 cells, J. Organomet. Chem. 700 (2012) 13–19, doi:10.1016/j.jorganchem.2011.10.036.

[4] R.P. Verma, Anti-cancer activities of 1,4-naphthoquinones: a QSAR study, Anticancer. Agents Med. Chem. 6 (2006) 489–499, doi:10.2174/187152006778226512.

[5] P. Ravichandiran, R. Kannan, A. Ramasubbu, Green synthesis of 1, 4-quinone derivatives and evaluation of their fluorescent and electrochemical properties, J. Saudi Chem. Soc. (2012) 1–7, doi:10.1016/j.jscs.2012.09.011.

[6] M. Mohamadi, S.Y. Ebrahimipour, J. Castro, M. Torkzadeh-mahani, Synthesis, characterization, crystal structure, DNA and BSA binding, molecular docking and in vitro anticancer activities of a mononuclear dioxido-uranium(VI) complex derived from a tridentate ONO aroylhydrazone, J. Photochem. Photobiol. B Biol. 158 (2016) 219–227, doi:10.1016/j.jphotobiol.2016.03.001.

[7] A. Satheshkumar, K. Ganesh, K.P. Elango, Charge transfer facilitated direct electrophilic substitution in phenylaminonaphthoquinones: experimental, theoretical and electrochemical studies, New J. Chem. 38 (2014) 993–1003, doi:10.1039/C3NJ01228J.

[8] P. Krishnamoorthy, P. Sathyadevi, R.R. Butorac, A.H. Cowley, N.S.P. Bhuvanesh, N. Dharmaraj, Copper(i) and nickel(ii) complexes with 1 : 1 vs. 1 : 2 coordination of ferrocenyl hydrazone ligands: Do the geometry and composition of complexes affect DNA binding/cleavage, protein binding, antioxidant and cytotoxic activities, Dalt. Trans. 41 (2012) 4423, doi:10.1039/c2dt11938b.

[9] T. Anand, G. Sivaraman, M. Iniya, A. Siva, D. Chellappa, Aminobenzohydrazide based colorimetric and 'turn-on' fluorescence chemosensor for selective recognition of fluoride, Anal. Chim. Acta. 876 (2015), doi:10.1016/j.aca.2015.03.035.

[10] C.D. Weber, C. Bradley, M.C. Lonergan, AIE active pyridinium fused tetraphenylethene: Rapid and selective fluorescent "turn-on" sensor for fluoride ion in aqueous media, J. Mater. Chem. 2 (2014) 303, doi:10.1039/x0xx00000x.

[11] S. Dhiman, M. Ahmad, N. Singla, G. Kumar, P. Singh, V. Luxami, et al., Chemodosimeters for optical detection of fluoride anion, Coord. Chem. Rev. 405 (2020) 213138, doi:10.1016/j.ccr.2019.213138.

[12] L. Gai, J. Mack, H. Lu, T. Nyokong, Z. Li, N. Kobayashi, et al., Organosilicon compounds as fluorescent chemosensors for fluoride anion recognition, Coord. Chem. Rev. 285 (2015) 24–51, doi:10.1016/j.ccr.2014.10.009.

[13] J. Jose, A. Sreekanth, A.M. John, S.M. Basheer, P.B. Sreeja, Spectrochemical and theoretical approaches for acylhydrazone-based fluoride sensors, Res. Chem. Intermed. 45 (2019) 425–435, doi:10.1007/s11164-018-3609-4.

[14] A. Kosiha, K.M. Lo, C. Parthiban, K.P. Elango, Studies on the interaction of mononuclear metal(II) complexes of amino-naphthoquinone with biomacromolecules, Mater. Sci. Eng. C. (2019), doi:10.1016/j.msec.2018.10.021.

[15] R. Selwin Joseyphus, M. Sivasankaran Nair, Synthesis, characterization and biological studies of some Co(II), Ni(II) and Cu(II) complexes derived from indole-3-carboxaldehyde and glycylglycine as Schiff base ligand, Arab. J. Chem. 3 (2010) 195–204, doi:10.1016/j.arabjc.2010.05.001.

[16] J. Tummachote, W. Punyain, S. Thanomsak, A. Sirikulkajorn, B. Tomapatanaget, Colorimetric N-butyl-3,6-diamidecarbazole-based chemosensors for detection of fluoride and cyanide anions, Spectrochim. Acta A Mol. Biomol. Spectrosc. 214 (2019) 384–392, doi:10.1016/j.saa.2019.02.081.

[17] O.E. Sherif, N.S. Abdel-Kader, Spectroscopic and biological activities studies of bivalent transition metal complexes of Schiff bases derived from condensation of 1,4-phenylenediamine and benzopyrone derivatives, Spectrochim. Acta Mol. Biomol. Spectrosc. 117 (2014) 519–526, doi:10.1016/j.saa.2013.08.037.

[18] N. Selvakumaran, N.S.P. Bhuvanesh, R. Karvembu, Self-assembled Cu(II) and Ni(II) metallamacrocycles formed from 3,3,3',3'-tetrabenzyl-1,1'-aroylbis(thiourea) ligands: DNA and protein binding studies, and cytotoxicity of trinuclear complexes, Dalton Trans 43 (2014) 16395–16410, doi:10.1039/c4dt01859a.

[19] R. Pegu, G. Pandit, A.K. Guha, S.K. Das, S. Pratihar, Selective detection of fluoride via amplified donor-acceptor interaction of 6H-indolo[2,3-b]quinoline, Spectrochim. A Mol. Biomol. Spectrosc. 211 (2019) 246–253, doi:10.1016/j.saa.2018.11.064.

[20] L. Mishra, A.K. Pandey, Coordination Behaviour of 1-(1-Phenyl-3-p-chlorophenyl)-pyrazolylcarboxaldehyde Thiosemicarbazone with Cobalt(II), Nickel(II), Copper(II) and Zinc(II), Synth. React. Inorg. Met. Chem. 21 (1991) 1–16, doi:10.1080/15533179108020162.

[21] J. Liu, X. He, J. Zhang, T. He, L. Huang, J. Shen, et al., A BODIPY derivative for colorimetric and fluorometric sensing of fluoride ion and its logic gates behavior, Sensors Actuators, B Chem. 208 (2015) 538–545, doi:10.1016/j.snb.2014.11.094.

[22] J. Ranjith Kumar, E. Rami Reddy, R. Trivedi, A.K. Vardhaman, L. Giribabu, N. Mirzadeh, et al., Isophorone-boronate ester: A simple chemosensor for optical detection of fluoride anion, Appl. Organomet. Chem. 33 (2019) 1–11, doi:10.1002/aoc.4688.

[23] V. Kumar, M.P. Kaushik, A.K. Srivastava, A. Pratap, V. Thiruvenkatam, T.N.G. Row, Thiourea based novel chromogenic sensor for selective detection of fluoride and cyanide anions in organic and aqueous media, Anal. Chim. Acta. 663 (2010) 77–84, doi:10.1016/j.aca.2010.01.025.

[24] A.S. Orabi, A.M. Abbas, S.A. Sallam, Spectral, magnetic, thermal, and DNA interaction of Ni(II) complexes of glutamic acid schiff bases, Synth. React. Inorganic, Met. Nano-Metal Chem. 43 (2013) 63–75, doi:10.1080/15533174.2012.684260.

[25] E. Jin, Y. Lee, H. Bae, Y. Ju, Novel azo dye-based color chemosensors for fluoride ions, Spectrochim. A Mol. Biomol. Spectrosc. 151 (2015) 655–661.

[26] Z.A. Tabasi, E.A. Younes, J.C. Walsh, D.W. Thompson, G.J. Bodwell, Y. Zhao, Pyrenoimidazolyl-Benzaldehyde Fluorophores: Synthesis, Properties, and Sensing Function for Fluoride Anions,, ACS Omega 3 (2018) 16387–16397, doi:10.1021/acsomega.8b02482.

[27] T. Ghosh, B.G. Maiya, M.W. Wong, Fluoride ion receptors based on dipyrrolyl derivatives bearing electron-withdrawing groups: Synthesis, optical and electrochemical sensing, and computational studies, J. Phys. Chem. A. 108 (2004) 11249–11259, doi:10.1021/jp0464223.

[28] D. Maity, A.K. Manna, D. Karthigeyan, T.K. Kundu, S.K. Pati, T. Govindaraju, Visible-near-infrared and fluorescent copper sensors based on julolidine conjugates: Selective detection and fluorescence imaging in living cells, Chem. - A Eur. J. 17 (2011) 11152–11161, doi:10.1002/chem.201101906.

[29] P. Anzenbacher, M.A. Palacios, K. Jursíková, M. Marquez, Simple electrooptical sensors for inorganic anions, Org. Lett. 7 (2005) 5027–5030, doi:10.1021/ol051992m.

[30] M.J. Frisch, G.W. Trucks, H.B. Schlegel, G.E. Scuseria, M.A. Robb, J.R. Cheeseman, J.A. Montgomery Jr., T. Vreven, K.N. Kudin, J.C. Burant, J.M. Millam, S.S. Iyengar, J. Tomasi, V. Barone, B. Mennucci, M. Cossi, G. Scalmani, N. Rega, G.A. Petersson, H. Nakatsuji, M. Hada, M. Ehara, K. Toyota, R. Fukuda, J. Hasegawa, M. Ishida, T. Nakajima, Y. Honda, O. Kitao, H. Nakai, M. Klene, X. Li, J.E. Knox, H.P. Hratchian, J.B. Cross, V. Bakken, C. Adamo, J. Jaramillo, R. Gomperts, R.E. Stratmann, O. Yazyev, A.J. Austin, R. Cammi, C. Pomelli, J.W. Ochterski, P.Y. Ayala, K. Morokuma, G.A. Voth, P. Salvador, J.J. Dannenberg, V.G. Zakrzewski, S. Dapprich, A.D. Daniels, M.C. Strain, O. Farkas, D.K. Malick, A.D. Rabuck, K. Raghavachari, J.B. Foresman, J.V. Ortiz, Q. Cui, A.G. Baboul, S. Clifford, J. Cioslowski, B.B. Stefanov, G. Liu, A. Liashenko, P. Piskorz, I. Komaromi, R.L. Martin, D.J. Fox, T. Keith, M.A. Al-Laham, C.Y. Peng, A. Nanayakkara, M. Challacombe, P.M.W. Gill, B. Johnson, W. Chen, M.W. Wong, C. Gonzalez, J.A. Pople, Gaussian, 03, Revision D.01, Gaussian, Inc., Wallingford CT, 2004.